Modelling of the toughening mechanisms in rubber-modified epoxy polymers

Part II *A quantitative description of the microstructure-fracture property relationships*

Y. HUANG, A. J. KINLOCH
Department of Mechanical Engineering, Imperial College of Science, Technology and Medicine, Exhibition Road, London SW7 2BX, UK

A mathematical model has been developed to quantify the relationships between the microstructure and fracture properties of multiphase rubber-toughened epoxy polymers. Good agreement between predictions from the model and experimental results have been found. The model also reveals that localized plastic shear banding in the epoxy matrix, running between the rubbery particles, is the dominating mechanism under all testing conditions. Plastic void growth in the epoxy matrix is the other main toughening mechanism. This latter mechanism is initiated by internal cavitation of the rubbery particle, or by debonding at the particle-matrix interface, and is particularly significant at higher test temperatures.

1. Introduction
An understanding of the relationships between the microstructure and fracture properties of crosslinked epoxy polymers toughened by the incorporation of a dispersed rubbery phase is of crucial importance if improved multiphase materials are to be developed. However, our appreciation of such relationships remains largely empirical and it is, therefore, highly desirable to develop mathematical models to enable the fracture properties to be predicted from the microstructural parameters and the basic mechanical properties of the materials forming the phases in the toughened thermosetting polymer.

Several models have been advanced in recent years. Kunz-Douglass *et al.* [1] developed a model which is based upon the energy dissipation during the stretching and bridging of the crack surfaces by rubber particles, i.e. termed the rubber-bridging mechanism. However, it is now generally accepted that rubber-bridging only plays a secondary role in the toughening of epoxy polymers. For example, this model failed to explain the phenomenon of stress whitening observed in most relatively tough rubber-modified epoxies.

Evans *et al.* [2] proposed a synergistic model which takes all the possible mechanisms, including rubber-bridging, void growth and shear banding, into consideration. However, the validity of this model has not yet been established due to the lack of experimental data. Moreover, the proposed synergistic relationship between the rubber bridging mechanism and the other two mechanisms was based on the assumption that the increase in the fracture energy, ΔG_{Ic}, scaled with the size of the process zone, r_y, i.e.

$$\Delta G_{\text{Ic}} = \beta r_y \tag{1}$$

where β is a constant. Although this relationship appears to be appropriate for the transformation toughening of ceramics [2], there has been no confirmation that it is valid for rubber-toughened polymers. Indeed, Yee [3] has cast doubts on the existence of synergism in the toughening mechanisms observed in rubber-toughened plastics. In a more recent model, Kinloch [4] calculated the increase in fracture toughness due to localized shear yielding inside the plastic zone. However, the contribution of plastic void growth of the epoxy matrix was not directly considered and the rubber bridging mechanism was not taken into account.

Obviously, a satisfactory model requires that the various energy-dissipating mechanisms are clearly identified and that their respective contributions to the increase in the fracture energy are quantified. Recent studies [1, 4-8] have provided a detailed description of the toughening mechanisms involved in the fracture of rubber-modified epoxy polymers. They include: (i) localized shear yielding, or shear banding, in the epoxy matrix which occurs between the rubbery particles [5, 6], (ii) plastic void, or hole, growth in the epoxy matrix which is initiated by cavitation or debonding of the rubbery particles [7, 8] and (iii) the rubber-bridging mechanism [1]. These mechanisms are schematically demonstrated in Fig. 1. The above studies form the necessary foundation for the development of a quantitative mathematical model.

2. The model
2.1. Introduction
The fracture energy of a rubber-toughened polymer may be expressed [4] by

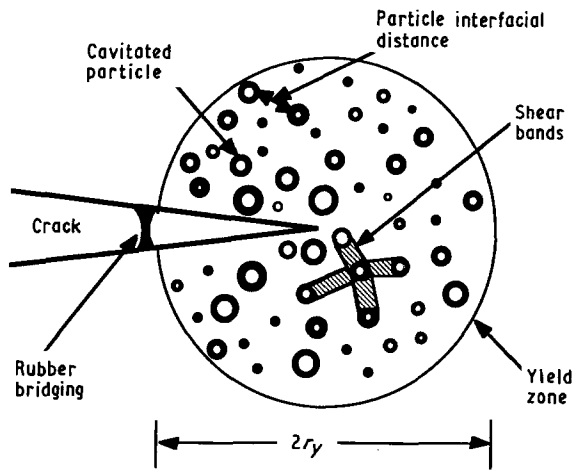$$G_{\text{Ic}} = G_{\text{Icu}} + \Psi \tag{2}$$

Figure 1 A schematic representation of the different toughening mechanisms involved in the fracture of multiphase rubber-toughened epoxy polymers. The diameter of the plastic, or process, zone is $2r_y$.

where G_{Icu} represents the fracture energy of the untoughened epoxy and Ψ represents the overall toughening contributions. Obviously, Ψ contains the contributions from the three different toughening mechanisms and can be separated into three terms

$$\Psi = \Delta G_s + \Delta G_v + \Delta G_r \qquad (3)$$

where ΔG_s, ΔG_v and ΔG_r represent the contributions to the overall increase in the fracture energy, G_{Ic}, from the localized shear banding, plastic void growth, and rubber-bridging mechanisms respectively.

Now ΔG_r may be evaluated via the model of Kunz-Douglass *et al.* [1]. The other two terms, ΔG_s and ΔG_v, are related to the size of the plastic zone and may be calculated from the following equation:

$$\Delta G_s \text{ or } \Delta G_v = 2 \int_0^{r_y} U(r)\,dr \qquad (4)$$

where r_y is the radius of the plastic zone ahead of the crack tip, r is the distance measured from the crack tip and $U(r)$ is the dissipated strain-energy density for the respective toughening mechanism; $U(r)$ has been denoted as $U_s(r)$ for the shear yielding mechanism and $U_v(r)$ for the plastic void growth mechanism. Further development of the model requires the evaluation of the size of plastic zone and the dissipated (or loss) strain-energy densities for the two toughening mechanisms.

2.2. Estimation of plastic zone size

From the concepts of linear elastic fracture mechanics (LEFM), the radius of the plastic zone, or process zone, is inversely proportional to the square of yield stress, as may be observed [9] from the following equation for the plane-strain case:

$$r_y = (1/6\pi)(K_1/\sigma_y)^2 \qquad (5)$$

where K_I is the stress intensity factor and σ_y is the yield stress. Assuming the plastic zone radii for the rubber-modified and the unmodified epoxies are r_y and r_{yu} respectively, then, to a first approximation

$$r_y/r_{yu} = (\sigma_{yu}/\sigma_c)^2 \qquad (6)$$

where σ_{yu} is the yield stress for the unmodified epoxy and σ_c is the critical stress for the rubber-modified material, as defined in Part I of the present paper [7]. The critical stress, σ_c, is the stress at which yielding starts in the matrix in the multiphase material and may be related to the yield stress of the matrix by

$$\sigma_{yu}/\sigma_c \equiv K_{vm} \qquad (7)$$

where K_{vm} is the maximum stress concentration factor of the von Mises stress in the plastic matrix. The value of K_{vm} may be calculated [7] from the finite-element method and represents the reduction in the effective yield stress. Combining the above two equations leads to

$$r_y/r_{yu} = K_{vm}^2 \qquad (8)$$

Equation 8 therefore predicts that the plastic zone size of a rubber-modified epoxy is increased by a factor equal to K_{vm}^2, due to the stress concentrations in the epoxy matrix around the rubber particles or voids. In the latter case, the voids are created by the internal cavitation of the dispersed rubbery particles, or debonding of the rubber particles from the matrix.

If there is no cavitation or debonding of the rubber particles followed by further void growth, then K_{vm} is the stress concentration factor caused only by the presence of the rubbery particles, and the calculations should be based upon the initial volume fraction, V_{fr} of rubbery particles. If, however, cavitation or debonding does occur and the voids continue to grow via plastic deformation of the epoxy matrix, the resultant volume fraction of voids, V_{fv}, will be higher than V_{fr}. The stress concentration factor increases with the volume fraction of rubber particles or voids, as reported [7] previously. Obviously, therefore, the stress concentrations in the epoxy matrix will be enhanced by the void growth process, and under such circumstances V_{fv} should be used to calculate the value of K_{vm}.

However, it is known that the yielding of glassy polymers is usually dependent on the hydrostatic stress component, and that the simple von Mises criterion is not strictly satisfied [10]. Instead, the von Mises criterion should be modified by

$$\tau_{vm} = \tau_y - \mu_m p \qquad (9)$$

where τ_{vm} is the von Mises shear stress, as defined in Equation 10, τ_y is the yield stress under pure shear, μ_m is a material constant and p is the hydrostatic stress. Thus

$$(\sigma_1 - \sigma_2)^2 + (\sigma_2 - \sigma_3)^2$$
$$+ (\sigma_3 - \sigma_1)^2 = 2\sigma_{vm}^2 = 6\tau_{vm}^2 \qquad (10)$$

and

$$p = \tfrac{1}{3}(\sigma_1 + \sigma_2 + \sigma_3)$$

where σ_{vm} is the von Mises tensile stress and the value of μ_m has been reported [11] to be between 0.175 and 0.225, and was taken to be 0.2. From Equation 9, it is

2764

obvious that the stress required for the material to shear yield under tensile loading is reduced. Hence, the relative size of the plastic zone will be increased. This increase can be described by an increase in K_{vm} by a factor of $(1 + \mu_m/3^{1/2})$, as derived in the Appendix. Therefore, Equation 8 has been modified to give

$$r_y = K_{vm}^2(1 + \mu_m/3^{1/2})^2 r_{yu} \qquad (11)$$

2.3. The contribution from the shear banding mechanism

As discussed earlier, it is necessary to ascertain the dissipated strain-energy density, $U_s(r)$, for the plastic shear banding mechanism to calculate the contribution to the increased toughness from this mechanism. Now the value of $U_s(r)$ may be assessed from

$$U_s(r) = V_{fm}(r) W_d(r) \qquad (12)$$

where $V_{fm}(r)$ is the volume fraction of the shear yielded matrix material inside the localized plastic-shear zone and $W_d(r)$ is the plastic strain-energy density of the matrix material. Both parameters are assumed to be functions of the radial distance, r, from the crack tip. These two parameters are discussed separately below.

2.3.1. Volume fraction of the shear yielded matrix material

The network of shear bands are schematically shown in Fig. 1, which is sketched from previous microscopic observations [4, 6]. Each rubbery particle has four shear bands associated with it, and these bands run between particles. A three-dimensional representation is given in Fig. 2 to illustrate the geometric relationships and, assuming a cubic array of particles, the average interfacial particle–particle distance, D_p, as defined in Fig. 2a, is given by

$$D_p = [(4\pi/3V_f)^{1/3} - 2]r_p \qquad (13)$$

where r_p is the radius of the rubbery particle or void and V_f equals V_{fr} or V_{fv}, depending on whether there has been any void growth. The number of particles or voids per unit volume may be defined by

$$N_v = 3V_f/(4\pi r_p^3) \qquad (14)$$

Next, assuming that the cross-sectional area of

a shear band scales with that diametrical cross-sectional of the particle or void, as in the case of rigid particulate-filled epoxy polymers [12], the cross-sectional area of a shear band, $A(r)$, is simply given by

$$A(r) = \alpha(r)\pi r_p^2 \qquad (15)$$

where $\alpha(r)$ is the scaling factor and is assumed to be a function of r. The length of a shear band $2L_s$, as defined in Fig. 2b, can then be expressed by

$$2L_s = 2r_p + D_p - 2[1 - \alpha(r)]^{1/2} r_p \qquad (16)$$

The volume of the shear bands per particle may then be calculated as:

$$V_m = n_s\{A(r)L_s - \tfrac{1}{3}\pi(L_s - \tfrac{1}{2}D_p)^2$$
$$\times [3r_p - (L_s - \tfrac{1}{2}D_p)]\} \qquad (17)$$

where n_s is the number of shear bands per particle, and is equal to four. Substituting Equations 13, 15 and 16 into Equation 17 leads to

$$V_m(r) = (\pi/6)n_s r_p^3 \{3(4\pi/3V_f)^{1/3}\alpha(r)$$
$$+ 4[1 - \alpha(r)]^{3/2} - 4\} \qquad (18)$$

The volume fraction of the shear yielded matrix material is then given by

$$V_{fm}(r) = V_m(r)N_v = 0.5 V_f\{3(4\pi/3V_f)^{1/3}\alpha(r)$$
$$+ 4[1 - \alpha(r)]^{3/2} - 4\} \qquad (19)$$

Now, the scaling factor was suggested by Kinloch [4] to be simply represented by

$$\alpha(r) = 1 - r/r_y \qquad (20)$$

The scaling factor, α, takes into account the strain field in the process zone and $1 \leq \alpha \leq 0$. Close to the crack tip the plastic strains will be relatively high and $\alpha \to 1$; at the edges of the process zone, where the strains approach the elastic limit $\alpha \to 0$. Thus, essentially, the variation in the value of α allows for the degree of shear yielding becoming more intense as the crack tip is approached.

2.3.2. The shear plastic strain-energy density

If the material is assumed to be perfectly elastic-plastic, then the shear plastic strain-energy density may then be defined by

$$W_d(r) = \tau_y \gamma(r) \qquad (21)$$

where τ_y and $\gamma(r)$ are the shear yield stress and the shear plastic strain of the matrix polymer.

Now for a material with the following macroscopic stress versus strain law:

$$\varepsilon = \varepsilon_y(\sigma_{vm}/\sigma_y)^n \qquad (22)$$

where n is the work hardening exponent, the strain fields near the crack tip were reported [13, 14] to be given by

$$\varepsilon_{ij} \sim r^{-n/(n+1)} \qquad (23)$$

where ε_{ij} are the components of the strain tensor. When $n \to \infty$, which corresponds to an elastic-perfectly-plastic material, Equation 23 becomes
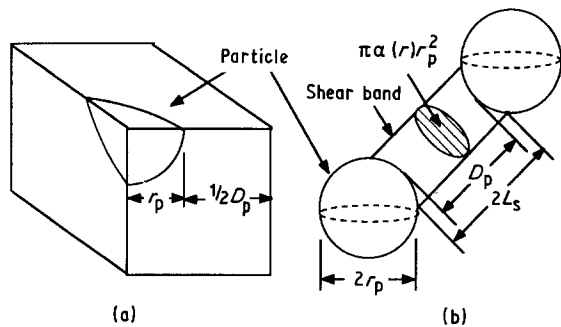
$$\varepsilon_{ij} \sim r^{-1} \qquad (24)$$

Figure 2 The three-dimensional geometric relationships. (a) The basic element used to represent the packing of rubbery particles. (b) The rubbery particles and a localized plastic shear band in the epoxy matrix.

The above equation states that for an elastic–perfectly-plastic material, the strain components scale with the inverse of the distance, r, inside the plastic zone. As a result, the following relationship may be assumed:

$$\gamma(r) = \gamma_f \alpha(r) \qquad (25)$$

where γ_f is the shear fracture strain of the matrix epoxy.

Thus the following expression for the shear plastic energy density may be obtained [10]:

$$W_d(r) = 0.5\sigma_{yc}\gamma_f\alpha(r) \qquad (26)$$

where σ_{yc} is the compressive yield stress of the matrix material, and values of σ_{yc} and γ_f may be determined by using the plane-strain compression test [4, 9, 15].

2.3.3. Evaluation of the increase in the fracture energy due to shear banding

By substituting Equations 19 and 26 into 12, the strain energy density arising from the shear banding mechanism may be calculated as

$$U_s(r) = 0.25 V_f \sigma_{yc}\gamma_f\alpha(r)\{3(4\pi/3V_f)^{1/3}\alpha(r)$$
$$+ 4[1 - \alpha(r)]^{3/2} - 4\}$$
$$= 0.25 V_f \sigma_{yc}\gamma_f f(r) \qquad (27)$$

where

$$f(r) = \alpha(r)\{3(4\pi/3V_f)^{1/3}\alpha(r) + 4[1 - \alpha(r)]^{3/2} - 4\} \qquad (28)$$

The increase in fracture energy due to the shear yielding mechanism, ΔG_s, may then be calculated by substituting Equations 27 and 28 into Equation 4 to obtain

$$\Delta G_s = 2\int_0^{r_y} U_s(r)\,dr = 0.5 V_f \sigma_{yc}\gamma_f F(r_y) \qquad (29)$$

where $F(r_y)$ may be expressed as

$$F(r_y) = \int_0^{r_y} f(r)\,dr = \int_0^{r_y} \left\{ 3\left(\frac{4\pi}{3V_f}\right)^{1/3}\alpha(r) \right.$$
$$\left. + 4[1 - \alpha(r)]^{3/2} - 4 \right\}\alpha(r)\,dr \qquad (30)$$

From Equation 20, then

$$d\alpha = -dr/r_y \qquad (31)$$

Substituting Equation 31 into 30 gives

$$F(r_y) = r_y\int_0^1 \left[3\left(\frac{4\pi}{3V_f}\right)^{1/3}\alpha^2 \right.$$
$$\left. + 4\alpha(1 - \alpha)^{3/2} - 4\alpha \right] d\alpha$$
$$= r_y[(4\pi/3V_f)^{1/3} - 54/35] \qquad (32)$$

Substituting Equations 11 and 32 into 29 leads to

$$\Delta G_s = 0.5(1 + \mu_m/3^{1/2})^2[(4\pi/3V_f)^{1/3}$$
$$- 54/35] V_f \sigma_{yc}\gamma_f r_{yu} K_{vm}^2 \qquad (33)$$

Considering the parameters in the above equation,

then the value of r_{yu} may be calculated from the fracture energy of the unmodified epoxy. V_f is the volume fraction of the initial rubbery particles, or the voided particles, and may be obtained directly from electron micrographs of the material, by using image analysis techniques if required [7, 8]. The values of σ_{yc} and γ_f may be measured by using the plane-strain compression test method [15] and K_{vm} may be calculated by using finite-element analysis [7], as described in Part I of the present studies.

2.4. The contribution from the plastic void growth mechanism

The increase of volumetric strain, $d\theta$, of a void during growth may be expressed as [2]

$$d\theta = V_f\,dV/V \qquad (34)$$

where V_f and V are the volume fraction and the average volume of the voids respectively. When a void grows from a volume of V_0 to V_1 the following relationship is valid if $V_f = V_{fr}$ at $V = V_0$ and $V_f = V_{fv}$ at $V = V_1$, namely:

$$V_f = V_{fr} + \frac{V_{fv} - V_{fr}}{V_1 - V_0}(V - V_0) \qquad (35)$$

Now, the strain-energy density for a void to grow from a volume of V_0 to V_1 is given by

$$U_v(r) = \int_{V_0}^{V_1} p\,d\theta \qquad (36)$$

where p is the local hydrostatic stress, or the local mean stress. The local hydrostatic stress may be assessed by using a schematic model proposed by Knott [16]

$$p = \sigma_{yt}(0.5 + r/a) \qquad (37)$$

where r is the distance from the crack tip, σ_{yt} is the tensile yield stress of the material, and a is the crack length. Assuming LEFM is valid

$$r \ll a \qquad (38)$$

Consequently, in the plastic zone

$$p \approx 0.5\sigma_{yt} \qquad (39)$$

Combining Equations 34 and 35 and then substituting these, and Equation 39, into 36 and integrating, yields

$$U_v(r) = 0.5\sigma_{yt}\left[V_{fv} - V_{fr} + \left(V_{fr} - \frac{V_{fv} - V_{fr}}{V_1/V_0 - 1} \right) \right.$$
$$\left. \times \log\left(\frac{V_1}{V_0}\right) \right] \qquad (40)$$

Assuming that

$$V_1/V_0 \equiv V_{fv}/V_{fr} \qquad (41)$$

then Equation 40 becomes

$$U_v(r) = 0.5\sigma_{yt}(V_{fv} - V_{fr}) \qquad (42)$$

Substituting Equation 42 into 4 and then integrating and substituting for r_y from Equation 11, the contribution to the increase in fracture energy from the plastic void growth mechanism is given by

$$\Delta G_v = (1 + \mu_m/3^{1/2})^2(V_{fv} - V_{fr})\sigma_{yt}r_{yu}K_{vm}^2 \qquad (43)$$

Again, V_{fr} and V_{fv} may be directly measured from the appropriate electron micrographs and the value of r_{yu} may be calculated from the fracture toughness of the unmodified epoxy. The value of K_{vm} may be determined by using the finite-element method [7]. Due to the effect of hydrostatic stress on the yield behaviour of glassy polymers, the tensile yield stress, σ_{yt}, is related to the compressive yield stress, σ_{yc}, by the following equation (see the Appendix):

$$\sigma_{yt} = \sigma_{yc}(3^{1/2} - \mu_m)/(3^{1/2} + \mu_m) \qquad (44)$$

Thus Equation 43 may be rewritten as

$$\Delta G_v = (1 - (\mu_m^2)/3)(V_{fv} - V_{fr})\sigma_{yc}r_{yu}K_{vm}^2 \qquad (45)$$

2.5. The contribution from the rubber-bridging mechanism

An equation to assess the contribution of the rubber-bridging mechanism has been proposed by Kunz-Douglass et al. [1] to be of the form

$$\Delta G_r = 4\Gamma_t(T)V_{fr} \qquad (46)$$

where V_{fr} is the volume fraction of rubbery particles and $\Gamma_t(T)$ is the tearing energy of the rubber particles. The tearing energy, $\Gamma_t(T)$, at room temperature for the dispersed rubbery phase used in the present studies was estimated [17] to be about $460 \pm 50\ \mathrm{J\,m^{-2}}$. These workers also undertook measurements at different test temperatures and the results are shown in Fig. 3. In the present study, the tearing energies at various temperatures will be obtained by interpolating or extrapolating the data shown in Fig. 3.

3. Application of the model

The value of Ψ may now be evaluated from Equations 3, 33, 45 and 46 to give

$$\Psi = 0.5(1 + \mu_m/3^{1/2})^2[(4\pi/3V_f)^{1/3} - 54/35]$$

$$\times V_f\sigma_{yc}\gamma_f r_{yu}K_{vm}^2 + (1 - (\mu_m^2)/3)(V_{fv} - V_{fr})$$

$$\times \sigma_{yc}r_{yu}K_{vm}^2 + 4\Gamma_t(T)V_{fr} \qquad (47)$$

The model may now be applied to a rubber-modified epoxy, which used 15 parts per hundred of resin (p.h.r.) of rubber (CTBN1300 × 8 rubber from BF Goodrich) and 5 p.h.r. piperidine as the hardener and was cured at 160 °C for 6 h. Details of this material have been described in detail elsewhere [8, 18]. The material properties needed to apply the model, such as the yield stress and the fracture strain, have been previously reported [18, 19] and are tabulated, to-

gether with the other parameters needed for the model, for a room temperature test and a displacement rate of $2\ \mathrm{mm\,min^{-1}}$ in Table I. Substituting these material properties into Equations 2 and 47, allows the fracture energy, G_{Ic}, for the rubber-modified epoxy polymer to be predicted under these test conditions. The measured value of $5.9\ \mathrm{kJ\,m^{-2}}$ compares very favourably with the predicted value of about $5\ \mathrm{kJ\,m^{-2}}$, especially when it is noted that there are no fitting terms in Equations 2 and 47.

Further, the very good predictive capability of the model is revealed when the effect of test temperature and rate on the value of G_{Ic} are considered. Fig. 4
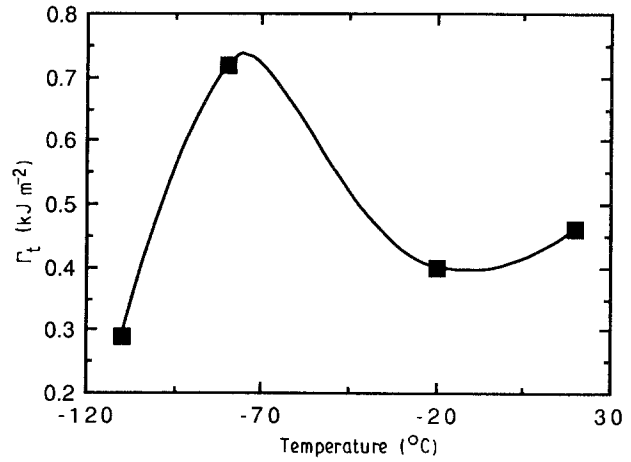
Figure 3 The tearing energy of the dispersed rubbery phase as a function of the test temperature (data from [17]).
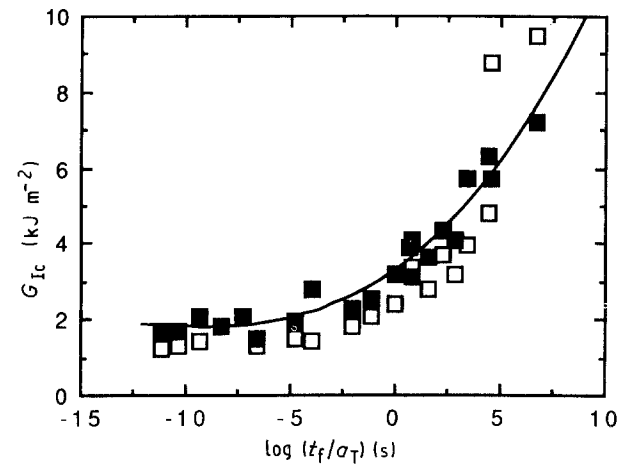
Figure 4 Comparison between the theoretical predictions from the ($\square$) model and the ($\blacksquare$) experimental results for the fracture energy, G_{Ic}, as a function of test temperature and rate of a rubber-toughened epoxy.

TABLE I Properties of the materials used in the model for test conditions of 23 °C and $2\ \mathrm{mm\,min^{-1}}$. The value of K_{vm} from Part I [7] was 4.54. The temperature and rate dependence of the properties E, σ_{yc}, γ_f, G_{Ic}, $\Gamma_t(T)$ and V_{fr} and V_{fv} were experimentally measured [7, 8, 17, 19]

Material	Modulus, E (GPa)	σ_{yc} (MPa)	γ_f	v	Fracture energy (kJ m^{-2})	V_{fr}	V_{fv}	r_p (μm)	T_g (°C)
Epoxy matrix	3.2	116	0.71	0.35	0.46	–	–	–	87
Rubbery phase	0.002	–	–	0.49	0.46	–	–	–	– 52
Rubber-toughened epoxy	–	–	–	–	–	0.19	0.27	1.6	89

shows the measured values of G_{Ic} for the rubber-toughened epoxy in the form of a master curve, where a_T is the time–temperature shift factor [4, 19–21] and tests were conducted over a range of test temperatures from $-60°$ to $40\,°C$ and displacement rates from 0.2 to $20\,mm\,min^{-1}$. Plane-strain compression tests were undertaken over a similar range of test conditions, to give E, σ_{yc} and γ_f as a function of the test conditions, and the surfaces of the fracture tests were examined to ascertain values of V_{fv}. Again the agreement between the predicted values of G_{Ic} and the experimentally measured values is very good.

The above model also allows the contributions from the different toughening mechanisms to be separated. Table II shows the proportional contributions to the total increase in the fracture energy from the three toughening mechanisms. Obviously, localized shear banding is the main toughening mechanism throughout the test temperature range. It constitutes more than 50% of the total dissipated energy, except when the temperature is relatively high at about $40\,°C$. At that temperature, the dominant proportion of the energy dissipation comes from the plastic void growth mechanism. In fact, the contribution of this mechanism increases sharply with temperature, i.e. from about 0% at $-40\,°C$ to 50% at $40\,°C$. An increase in the test temperature causes a decrease in the yield stress of the matrix material and the ability for voids to grow in the matrix is subsequently enhanced. The rubber-bridging mechanism only plays a minor role. However, note that the contribution from the plastic void growth may be completely suppressed at low test temperatures. Under such conditions, the overall increase in toughness is small and the rubber-bridging mechanism makes a higher proportional contribution to the overall toughness.

These data emphasize the importance of not only attaining the required microstructure, which consists of a dispersed rubbery phase in the thermosetting matrix, but also the ability of the thermosetting matrix to undergo plastic deformation. High test temperatures and low test rates, when the matrix can undergo plastic yielding more readily, lead to higher values of G_{Ic}. However, other factors such as the chemical backbone structure and degree of crosslinking of the matrix will obviously affect the ability of the matrix to plastically deform [18, 22] and so affect the toughness of the rubber-modified polymer.

4. Conclusions

A mathematical model has been developed to quantify the relationships between the microstructure and the

fracture properties in rubber-toughened epoxy polymers. Predictions from the model are in good agreement with experimental results. For the multiphase polymer currently studied the model also reveals that, at room and low test temperatures, the localized shear yielding which is initiated by the rubbery particles and runs between particles is a major toughening mechanism. The plastic void growth is another main toughening mechanism at higher test temperatures, and its contribution increases sharply with rising temperature. The rubber bridging mechanism can also play a role when the ability of the matrix to undergo plastic deformation is suppressed.

Appendix

The yield behaviour of glassy polymers is typically dependent upon the hydrostatic stress component, p. Thus in the proposed model we need take this feature into account.

Firstly, the stress concentrations around a rubbery particle were calculated in Part I [7] by using a numerical finite-element analysis methods for a two-dimensional plane-strain model which was subjected to uniaxial loading. Thus the equivalent or von Mises stress is given by

$$\sigma_{vm} = \{0.5[(\sigma_1 - \sigma_2)^2 + (\sigma_2 - \sigma_3)^2 + (\sigma_3 - \sigma_1)^2]\}^{0.5} \approx \sigma_1 \qquad (A1)$$

and

$$p = (\sigma_1 + \sigma_2 + \sigma_3)/3 \approx \sigma_1/3 \approx \sigma_{vm}/3 \qquad (A2)$$

Now from Equation 10 we have

$$\sigma_{vm} = 3^{1/2}\tau_{vm} \qquad (A3)$$

hence

$$p = \tau_{vm}/3^{1/2} \qquad (A4)$$

Substituting Equation A4 into Equation 9, leads to

$$\tau_{vm} = \tau_y/(1 + \mu_m/3^{1/2}) \qquad (A5)$$

The implication of Equation A5 is that the effective yield stress of a polymer is reduced by a factor of $(1 + \mu_m/3^{1/2})$ due to the dependence of the yield process on the hydrostatic stress component. This factor is therefore incorporated into Equation 11.

Secondly, the dependence of the yield process on the hydrostatic stress also leads to the yield stress being different in tension and compression. For uniaxial tension:

$$\sigma_{yt}/3^{1/2} = \tau_0 - \mu_m\sigma_{yt}/3 \qquad (A6)$$

while for compression, assuming the uniaxial and

TABLE II The proportional contributions to the increase in the fracture energy of the rubber-modified epoxy due to the three toughening mechanisms. G_{Ic} was measured at a displacement rate of $2\,mm\,min^{-1}$.

Temperature (°C)	− 60	− 40	− 20	0	23	40
G_{Ic} (kJ m^{-2})	1.72	1.96	2.53	3.64	5.90	7.23
G_{Ic} (kJ m^{-2}) (model)	1.30	1.49	2.05	2.72	4.79	8.25
$\Delta G_s/\Psi$	0.64	0.74	0.68	0.60	0.54	0.47
$\Delta G_v/\Psi$	0.00	0.00	0.18	0.29	0.38	0.48
$\Delta G_r/\Psi$	0.36	0.26	0.14	0.11	0.08	0.05

plane-strain compressive yield stresses to be very similar in value

$$\sigma_{yc}/3^{1/2} = \tau_0 + \mu_m \sigma_{yc}/3 \qquad (A7)$$

and combining Equations A6 and A7 leads to the relationship

$$\sigma_{yt} = \sigma_{yc}(3^{1/2} - \mu_m)/(3^{1/2} + \mu_m) \qquad (44)$$

Acknowledgements

References

1. S. KUNZ-DOUGLASS, P. W. R. BEAUMONT and M. F. ASHBY, *J. Mater. Sci.* **15** (1980) 1109.
2. A. G. EVANS, Z. B. AHMAD, D. G. GILBERT and P. W. R. BEAUMONT, *Acta Metall.* **34** (1986) 79.
3. A. F. YEE, in "Polymer blends: conference proceedings" (Plastics and Rubber Institute, London, 1990) p. EK1/1.
4. A. J. KINLOCH, in "Rubber-toughened plastics", edited by C. K. Riew, Advances in Chemistry Series, vol. **222** (American Chemical Society, Washington, D.C., 1989) p. 67.
5. A. J. KINLOCH, S. J. SHAW and D. L. HUNSTON, *Polymer* **24** (1983) 1355.
6. R. A. PEARSON and A. F. YEE, *J. Mater. Sci.* **21** (1986) 2475.
7. Y. HUANG and A. J. KINLOCH, *J. Mater. Sci.* **27** (1992) 2753.
8. *Idem.*, *J. Mater. Sci. Lett.*, in press.
9. A. J. KINLOCH and R. J. YOUNG, "Fracture behaviour of polymers" (Applied Science Publishers Ltd, London, 1983).
10. P. B. BOWDEN, in "The physics of glassy polymers", edited by R. N. Haward (Applied Science Publishers Ltd, London, 1975).
11. J. N. SULTAN and F. J. McGARRY, *Polymer Engng Sci.* **13** (1973) 29.
12. J. W. SMITH, "Deformation induced failure mechanisms in particulate filled epoxy resins", PhD thesis, Ecole Polytechnique Federale de Lausanne (1989).
13. J. R. RICE and G. F. ROSENGREN, *J. Mech. Phys. Solids* **16** (1968) 1.
14. J. W. HUTCHINSON, *J. Mech. Phys. Solids* **16** (1968) 13.
15. J. G. WILLIAMS and H. FORD, *J. Mech. Engng Sci.* **6** (1964) 7.
16. J. F. KNOTT, "Fundamentals of fracture mechanics" (Butterworths, London, 1979).
17. S. C. KUNZ and P. W. R. BEAUMONT, *J. Mater. Sci.* **16** (1981) 3141.
18. A. J. KINLOCH, C. A. FINCH and S. HASHEMI, *Polymer Commun.* **28** (1987) 229.
19. Y. HUANG, "Microstructure-property relationships in toughened epoxy polymers", PhD thesis, University of London (1991).
20. D. L. HUNSTON, A. J. KINLOCH, S. J. SHAW and S. S. WANG, "Adhesive joints", edited by K. L. Mittal (Plenum Press, New York, 1984) p. 789.
21. D. L. HUNSTON and G. W. BULLMAN, *Int. J. Adhesion Adhesives* **5** (1985) 69.
22. R. A. PEARSON and A. F. YEE, *J. Mater. Sci.* **24** (1989) 2571.